



## Original Research Article

# Synthesis and Characterization of Chrome (VI) Ion/Iron Oxide/Chitosan Composite for Oxidation of Methylene Blue by Photo-Fenton Reaction

Yaman Khalid Sadiq\* , Khulood A. Saleh

Department of Chemistry, College of Science, Baghdad University, Iraq

### ARTICLE INFO

#### Article history

Submitted: 2022-07-13

Revised: 2022-08-16

Accepted: 2022-10-24

Manuscript ID: CHEMM-2209-1608

Checked for Plagiarism: Yes

Language Editor:

Dr. Nadereh Shirvani

Editor who approved publication:

Dr. Lotf Ali Saghatforoush

DOI:10.22034/CHEMM.2022.361921.1608

### KEYWORDS

Degradation

Adsorption

MB dye

CS/Fe<sub>3</sub>O<sub>4</sub> composite

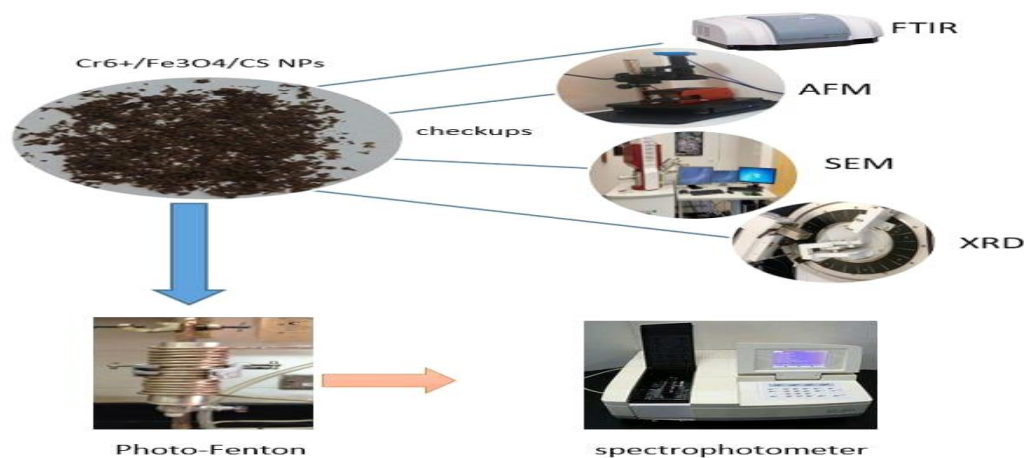
AFM

BET

### ABSTRACT

Removing heavy metal ions from organic contaminants by industrial wastewater treatment systems is a difficult challenge. In this study, organic contaminants were degraded using functional composite hydrogels with photo-Fenton reaction activity. Chromium, chitosan, Fe<sub>3</sub>O<sub>4</sub>, and other ingredients go into the making of the hydrogel. Following are some factors that changed photo-Fenton activity: (pH, H<sub>2</sub>O<sub>2</sub> conc., temp, and exposure period). AFM was used to analyze the composite's morphology and typical diameter (AFM). It investigated how much chromium adsorbs on chitosan (BET). After 60 minutes of UV exposure, The MB dye degradation in the Cr<sup>6+</sup>/Fe<sub>3</sub>O<sub>4</sub>/CS hydrogel composite was 90.4%.

### GRAPHICAL ABSTRACT



\* Corresponding author: Yaman Khalid Sadiq

✉ E-mail: [yaman.khaled1205m@sc.uobaghdad.edu.iq](mailto:yaman.khaled1205m@sc.uobaghdad.edu.iq)

© 2023 by SPC (Sami Publishing Company)

## Introduction

The traditional Fenton reaction, used to treat wastewater, is an example of an advanced oxidation technology. In this reaction, ferrous iron ( $\text{Fe}^{2+}$ ) and hydrogen peroxide ( $\text{H}_2\text{O}_2$ ) are combined to produce hydroxyl radicals ( $\text{OH}$ ) [1]. Homogeneous Fenton reactions have a number of drawbacks, including an acidic pH, efficient  $\text{H}_2\text{O}_2$  consumption, and the production of sludge [2]. These drawbacks limit their potential applications. A big  $\text{H}_2\text{O}_2$ - $\text{Fe}^{2+}$  molar ratio and the requirement for a lot of  $\text{Fe}^{2+}$  further raise the requirement for reagents [3]. For the degradation of organic pollutants, the heterogeneous Fenton reaction employs solid, iron-containing compounds or solid materials rich in iron, including clay [4], mesoporous silica [5], and activated carbon [6], supported iron-containing compounds,  $\text{Fe}_3\text{O}_4$  [7, 8],  $\text{Fe}_2\text{O}_3$  [9]. Comparatively, the heterogeneous Fenton reactions are a successful oxidative method used to destroy organic contaminants that can effectively enhance  $\text{H}_2\text{O}_2$  conversion with little breakdown, the preparation of hydrogels with exceptional mechanical characteristics was motivated by high attendance [10]. In order to make a hydrogel with high strength, there are typically three different recipes: a topological gel [11], a double network gel [12], and a composite gel [13]. Composite gels are among these recipes and are thought to improve the mechanical properties of hydrogels; for example, composite gels with a special organic-inorganic network structure would have extraordinary mechanical properties [14]. UV addition to the Fenton process may be a crucial ally in the decolorization of dye due to its capacity to impact the direct production of  $\text{OH}$  radicals. The photo Fenton procedure, which involves exposing Fenton to UV light, may accelerate the degradation of organic pollutants. By reducing  $\text{Fe}^{3+}$ , UV light also encourages the recycling of ferrous catalyst and increases the formation of hydroxyl radicals. By using this method,  $\text{Fe}^{2+}$  concentrations will increase, and the reaction as a whole will accelerate. AOPs' dye degradation and

decolorization have been successfully treated with oxidation using photo-Fenton and Fenton reagents [15]. Fenton's reagent, based on ferrous ion and hydrogen peroxide, is used to oxidize material by taking advantage of the hydroxyl radicals produced in an acidic solution as a result of the catalytic breakdown of  $\text{H}_2\text{O}_2$  [16]. *Chitosan* is a water-soluble polymer and is widely used in industrial water treatment. It is treated as non-toxic, economical, and efficient and undoubtedly has great potential application prospects. CS is a low-cost bio-adsorbent and disinfectant with a number of advantages, including the amine functional group, which is totally reactive among metal ions, biocompatibility, biodegradability, and the safety of their use due to their non-toxic behavior [17]. The hydrogels  $\text{Cr}^{6+}/\text{Fe}_3\text{O}_4/\text{CS}$  is efficient to adsorb heavy metals this is because of the chemical adsorption ascribed to the metal  $\text{NH}_2$  complex.

## Materials and Methods

### *Determination of maximum absorption ( $\lambda_{max}$ )*

The amount of MB absorption was calculated using the wavelength value of 661 nm, as shown in Figure 1. MB dye was chosen as a measure to study the surface area to know the rate of degradation through photo Fenton reaction and consider the dye as a pollutant instead of polluted water. An ultraviolet visible absorption spectrum was performed for MB blue. The absorption spectrum is shown as peaks between absorbance and wavelength.

Figure 2 illustrates the calibration curve used to determine a linear equation using Beer-law Lambert's to determine a substance's concentration and the relationship between concentration and absorbance.

### *Synthesis of CS/ $\text{Fe}_3\text{O}_4$ nanocomposite*

Chitosan in 1% acetic acid solution and stirring was dissolved continuously for 10 minutes to create well-oxidized nanocomposites via the Fenton reaction.

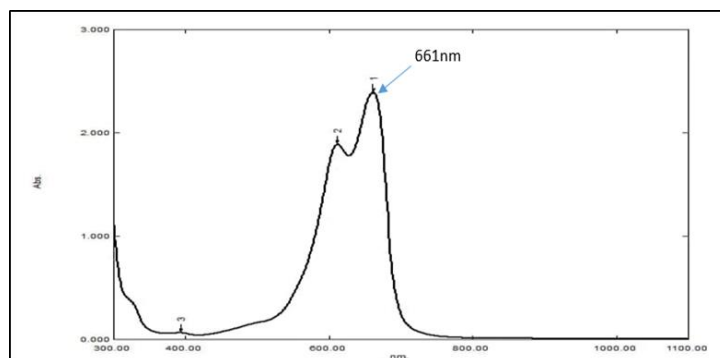


**Figure 1:** The absorption spectrum for M.B. dye by UV-Vis

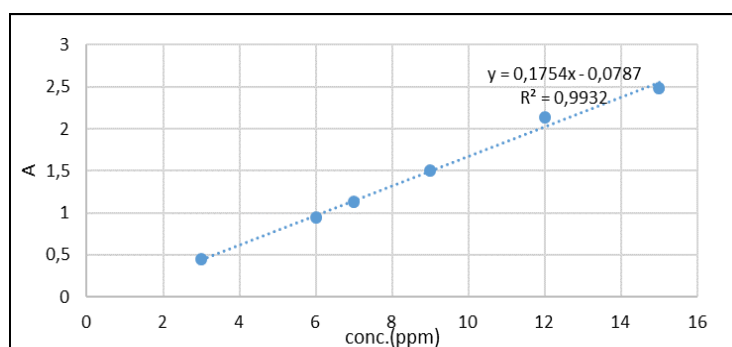


**Figure 2:** Calibration curve of MB

Iron oxide was added once the suspension was well-suspended. The solution was then thoroughly mixed up in an ultrasonic device for 4 minutes to ensure no agglomeration of the particles. This is carried out at 20 °C. After that, we gradually add the ammonium hydroxide solution and put the mixture back into the ultrasonic device to create a homogeneous solution of the magnetic compound. We then allow it to dry for 24 hours, as indicated in Figure 3, a magnetic crystalline powder is obtained, and this powder is dissolved and added to a 20-ppm chromium solution before the mixture is added to the Fenton cell [18].

Figure 4 and 5 show the interaction of chromium and iron oxide with chitosan through Fourier Transform Infrared spectroscopy (FT-IR) due to the shift of all peaks and the appearance of new peaks between 400-800  $\text{cm}^{-1}$ , indicating the interaction of one of the transition elements, which is chrome with the original compound.

#### *Preparation of photocell*

A stainless-steel tube with a diameter of 4 cm and a length of 15 cm was outfitted with a copper coil around the outer cell surface and connected to a water bath to control the reactor heat and lamp. First, the inner cell surface is treated with concentrated HF acid, producing the inside of the cell or photo that is also rough and could take up paint. After 10 minutes, the Fenton-filled reactor Cr/Fe<sub>3</sub>O<sub>4</sub>/CS compound suspension is decanted to allow a stable coating layer to form [19]. For the purpose of impregnating the Cr/Fe<sub>3</sub>O<sub>4</sub>/CS catalyst photo reactor layer. In order to increase the efficiency of the cell's ability to oxidize well, it is exposed to 500 °C until the inner surface is compressed with the compound. Repeat these steps several times to make the coating more than one layer, and the presence of catalysts for the reaction, such as hydrogen peroxide, is added to the dye to test the coating's stability. Figure 6 displayed the equipment for the degrading process and the suspension composite covering the cell.

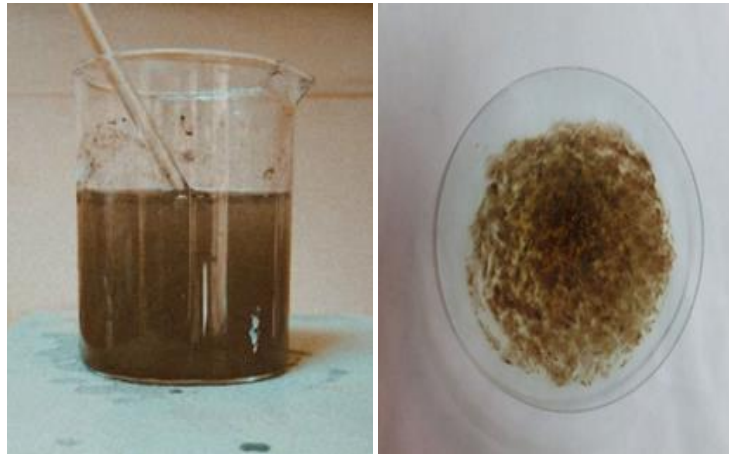


Figure 3: Cr<sup>6+</sup>/Fe<sub>3</sub>O<sub>4</sub> /CS composite

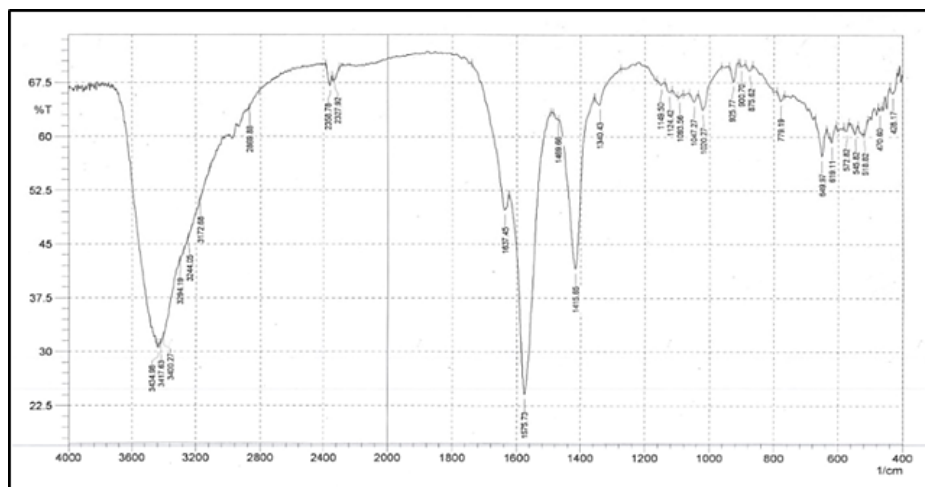


Figure 4: The FT-IR spectrum of chitosan

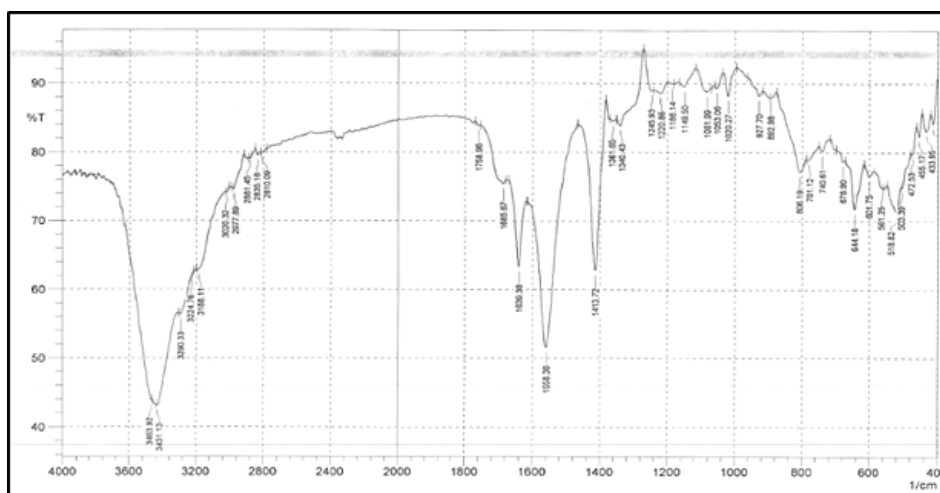
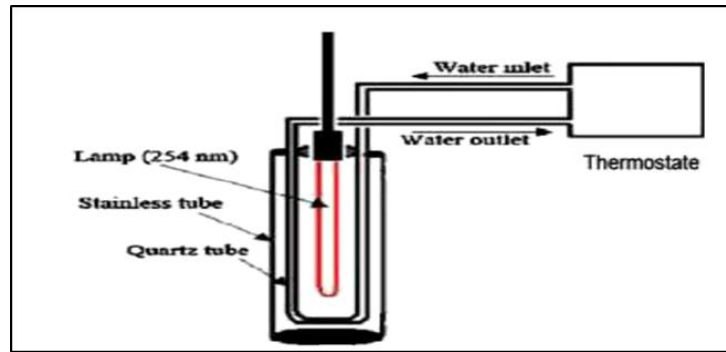


Figure 5: The FT-IR spectrum of Cr<sup>6+</sup>/ Fe<sub>3</sub>O<sub>4</sub> /CS composite



**Figure 6:** Shows how to set up the entire system for photo degradation

## Results and Discussion

### Atomic force microscope

According to the AFM investigation, the composite of  $\text{Cr}^{6+}$ ,  $\text{Fe}_3\text{O}_4$ , and CS has measurements for its average grain size and granularity cumulating distribution. The parameters average roughness ( $S_a$ ) and square roughness are the most often utilized ( $S_q$ ). The data of  $\text{Cr}^{6+}/\text{Fe}_3\text{O}_4/\text{CS}$  were (roughness average=7.400, root mean square=8.496, surface skewness=-0.2388, average diameter=12.66) nm. As shown in [Figure 7](#).

### Brunauer-emmett-teller (BET)

A theoretically valid isotherm equation for the equilibrium of gas-solid systems is Brunauer-Emmett-Teller. The multilayer adsorption theory (BET), developed as an extension of the Langmuir technique, stipulates that there is a dynamic

equilibrium between adsorbate molecules in succeeding layers, and adsorbed molecules may condense on it after the development of a molecular monolayer [20]. They provide the equation commonly referred to as the BET (Equation 1), which:

$$\frac{p}{V(P_0 - P)} = \frac{1}{V_m C} + \left(\frac{C-1}{V_m C}\right) \frac{P}{P_0} \quad (1)$$

The BET specific surface area ( $a_s$ ) calculated from the BET plots for the adsorption of  $\text{Cr}^{6+}$  ion onto CS or CS/ $\text{Fe}_3\text{O}_4$ . The  $a_s$ , BET increased from 2.7269  $\text{m}^2 \text{g}^{-1}$  for CS to 6.5481  $\text{m}^2 \text{g}^{-1}$  for CS/ $\text{Fe}_3\text{O}_4$  and 12.5032  $\text{m}^2 \text{g}^{-1}$  for  $\text{Cr}^{6+}/\text{Fe}_3\text{O}_4/\text{CS}$  indicates that when  $\text{Fe}_3\text{O}_4$  is added to CS, the surface area of CS/ $\text{Fe}_3\text{O}_4$  increases, when  $\text{Cr}^{6+}$  ion was added to CS/ $\text{Fe}_3\text{O}_4$  composite, the surface area was significantly increased as shown in [Figure 8](#) and [9](#).

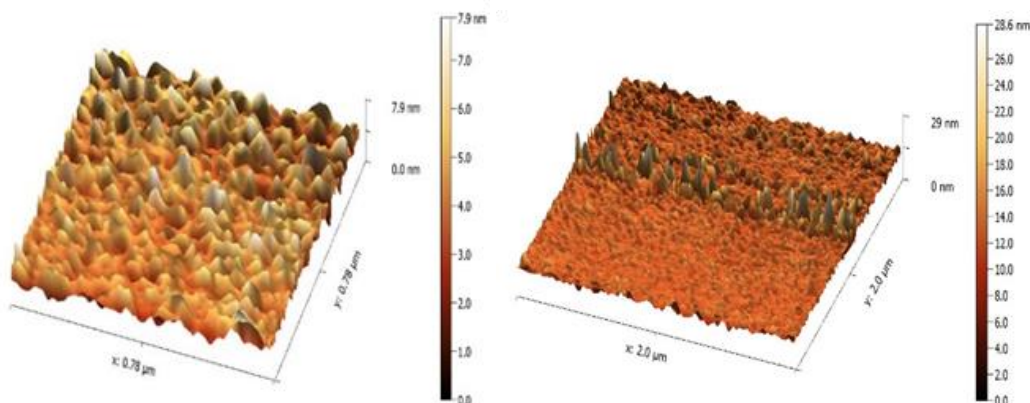


**Figure 7:** AFM images for  $\text{Cr}^{6+}/\text{Fe}_3\text{O}_4/\text{CS}$

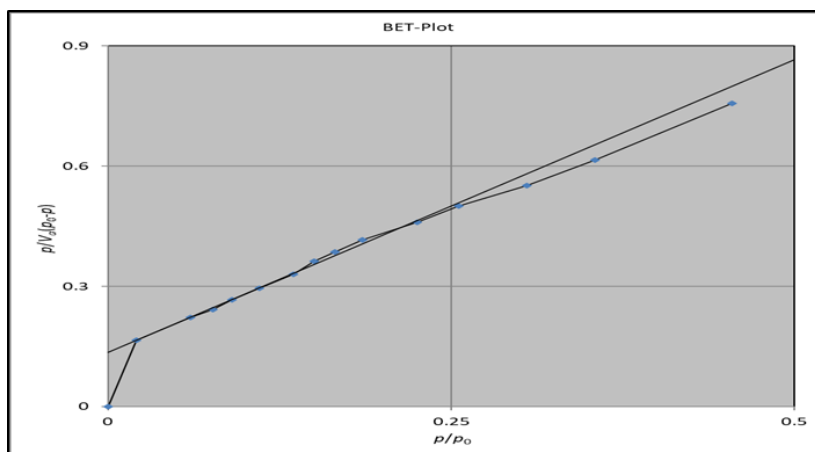


**Figure 8:** BET plots of CS adsorption isotherms

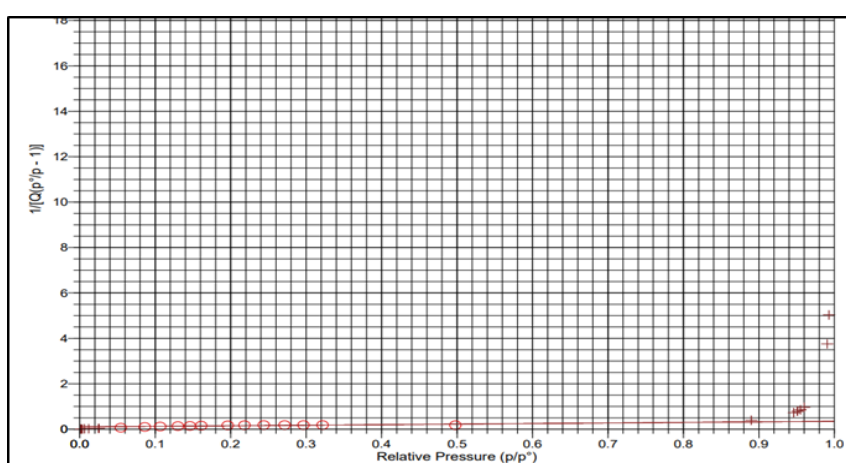


**Figure 9:** BET plots of  $\text{Cr}^{6+}/\text{Fe}_3\text{O}_4/\text{CS}$  adsorption isotherms

#### *Effect of $\text{H}_2\text{O}_2$ concentration*

The concentration of hydrogen peroxide is one of the operational parameters that significantly influences the ultimate mineralization extent. Degradation efficiency also rises with further increases in the optimal Fenton reagent ratio when a particular point is achieved ( $\text{H}_2\text{O}_2$  conc.). At 298 K, pH=7 after 60 min in the presence of catalyst CS,  $\text{Cr}^{6+}/\text{Fe}_3\text{O}_4/\text{CS}$  composite, the impact of  $\text{H}_2\text{O}_2$  conc. on the MB degradation was investigated, and the rise in % deg. [21] with  $\text{H}_2\text{O}_2$  conc. increased, as shown in Figure 10.

#### *Effect of $\text{Cr}^{6+}$ ion concentration*

After 60 minutes, in the presence of CS and  $\text{Cr}^{6+}/\text{Fe}_3\text{O}_4/\text{CS}$ , hydrogen peroxide ( $5 \times 10^{-3}\text{M}$ ), the chromium ion concentration affected the percentage of MB at 7 ppm. In order to maintain

stable levels of the dye solutions in the compounds, the photolysis method was carried out at pH 7 and 298 K. The location where the dye-pollutant mixture and chromium solution were combined. The degradation rate was greater than that of chitosan with the combination  $\text{Cr}^{6+}/\text{Fe}_3\text{O}_4/\text{CS}$ . Figure 11 illustrates that 20 ppm of chromium was the ideal amount to employ in this operation.

#### *Effect of temperature*

The effects of temperature on the degradation of MB dye have been studied using  $\text{Cr}^{6+}/\text{Fe}_3\text{O}_4/\text{CS}$  composite, MB dye (7 ppm),  $\text{H}_2\text{O}_2$  concentration ( $5 \times 10^{-3}\text{M}$ ), pH=7, and temperatures of (293, 303, 313 and 323) K. Following then, samples were taken every 5 minutes; after UV exposure. Figure 12 demonstrates the determination of %deg.

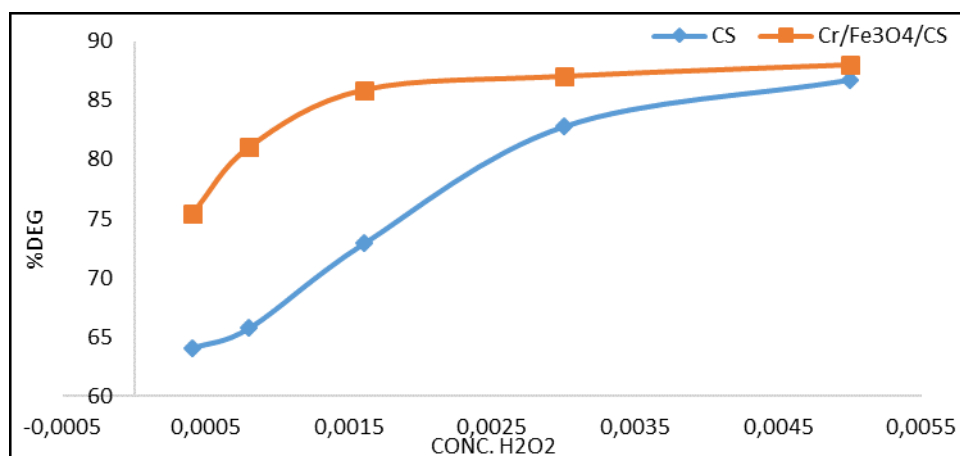


**Figure 10:** Shows the catalyst effect of varied H<sub>2</sub>O<sub>2</sub> conc. for (7 ppm M.B) after 60 min at 298K, pH=7

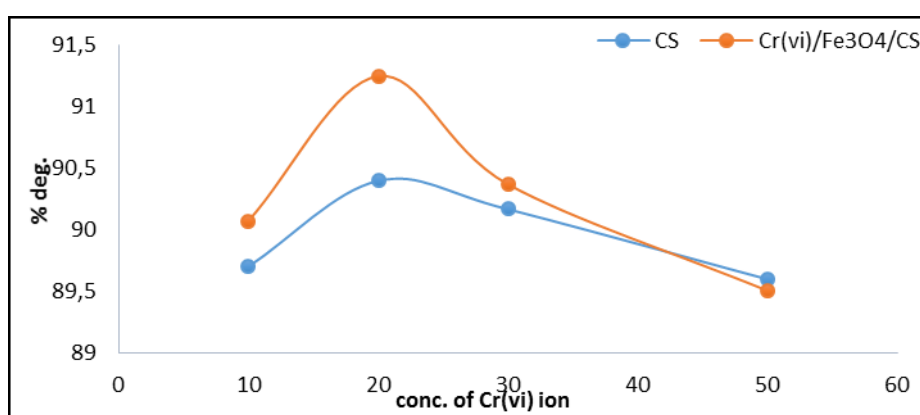


**Figure 11:** Shows the impact of changing the Cr<sup>6+</sup> ion concentration for M.B. (7ppm) concentration, 5×10<sup>-3</sup> (H<sub>2</sub>O<sub>2</sub> conc.) after (60 min.), at 298K, pH=7 on the CS, Cr/Fe<sub>3</sub>O<sub>4</sub>/CS compound catalyst

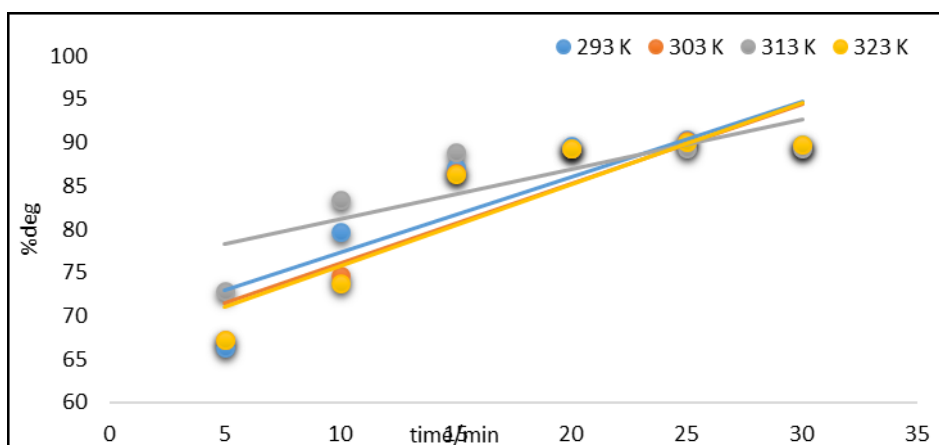


**Figure 12:** Shows how the temperature-dependent variation of 7 ppm M.B with (5×10<sup>-3</sup> H<sub>2</sub>O<sub>2</sub> conc.), %deg. by Cr<sup>6+</sup>/Fe<sub>3</sub>O<sub>4</sub>/cs composite

#### Kinetic degradation study

The first order was applied to the deteriorating reaction of 7 ppm M.B and 5×10<sup>-3</sup> M of H<sub>2</sub>O<sub>2</sub> using a CS/Fe<sub>3</sub>O<sub>4</sub> composite. At a pH of 7, the connection

between temperature and degradation rate was examined. It could be fitted into relation curves, showing the first-order kinetics of the reaction as

given in the following (Equation 2) [22]. Figure 13 displays kinematic calculations by  $\ln C_t$  and time.

$$\ln C_t = \ln C_0 - Kt \quad (2)$$

Where:  $C_0$ : initial concentration of M.B,  $C_t$ : concentration of M.B after exposing to UV at time,  $K$ : rate constant and  $t$ : time.

The anti-arrhenius equation was applied to determine the kinetic parameter  $A$ ,  $E_a$ , as shown in Figure 14: (Equations 3 and 4) [23].

$$k = A \exp (E_a/RT) \quad (3)$$

$$\ln k = \ln A + E_a/RT \quad (4)$$

Where  $T$ : is the absolute temperature (measured in kelvins),  $k$  is the rate constant,  $E_a$  is the reaction's activation energy (measured in kilojoules per mole),  $A$  is the pre-exponential factor, and  $R$  is the universal gas constant. In the rate equation,  $E_a$  stands for the activation of degradation (the least amount of energy needed to initiate a chemical process).  $A$  stands for the pre-exponential component. The values of  $E_a$  and  $A$  are then determined by the slope and intercept of the  $\ln k$  against the  $1/T$  plot, respectively, and are shown in Table 1.

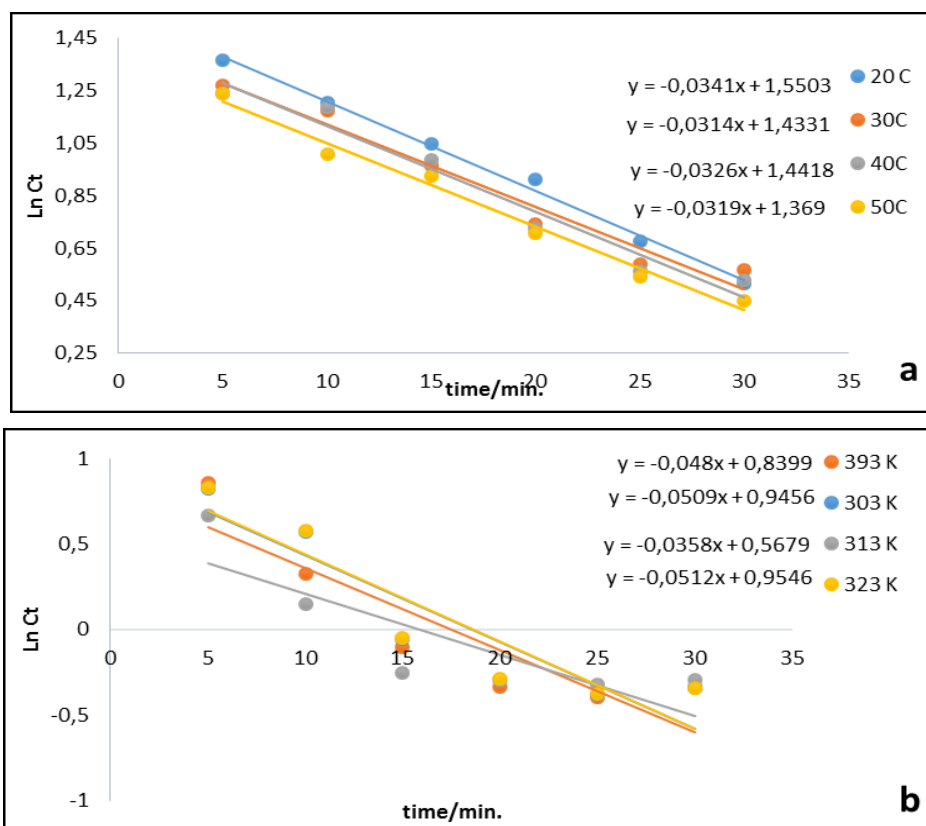


**Figure 13:** linear relations between  $\ln C_e$  and time for (7 ppm M.B deg.) by a) CS, B)  $Cr^{6+}/Fe_3O_4/CS$  composite at different temperatures

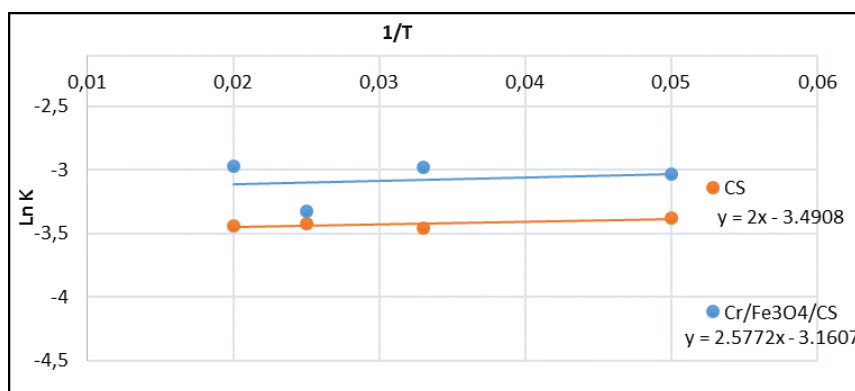


**Figure 14:** Anti-arrhenius plots, relation  $\ln k$  with  $1/T$  for the 7 ppm M.B %deg. CS coating, Cr/Fe<sub>3</sub>O<sub>4</sub>/CS composite

**Table 1:** Kinetic parameters for the materials CS and CS/Fe<sub>3</sub>O<sub>4</sub> composite

Metal	T(K)	$k/(\text{min.}) \times 10^3$	$\ln k$	$E_a/\text{kmol}^{-1}$	$A(\text{min}^{-1})$
	293	0.0341	-3.378		
CS	303	0.0314	-3.461	16.628	0.031
	313	0.0326	-3.423		
	323	0.0319	-3.445		
	293	0.048	-3.036		
Cr <sup>6+</sup> /Fe <sub>3</sub> O <sub>4</sub> /CS	303	0.0509	-2.977	21.427	0.042
	313	0.0358	-3.328		
	323	0.0512	-2.972		

## Conclusion

The absorption spectrum and calibration curve of methyl blue were performed as illustrated in Figure 1 and 2. The degradability of methylene blue dye on composites made of Cr, Fe<sub>3</sub>O<sub>4</sub>, and CS was investigated. By manufacturing Cr<sup>6+</sup>/Fe<sub>3</sub>O<sub>4</sub>/CS nanocomposite as shown in the Figure 3 on the research method [24] to break down the pollutants dye (Methyl blue). The composite's characteristics, such as its typical diameter and shape, were determined using AFM. Additionally, BET was used to determine the Fe<sub>3</sub>O<sub>4</sub> composite's surface area for chromium ion adsorption. When Cr ions are combined with CS/Fe<sub>3</sub>O<sub>4</sub>, which was diagnosed by FT-IR as in the given Figure 5, the particle size increases, and MB (% deg.) efficiency rises. The photo-Fenton approach successfully removed the contaminating dye using a Cr<sup>6+</sup>/Fe<sub>3</sub>O<sub>4</sub>/CS composite as a catalyst. The ideal exposure period was found to be 60 minutes. The pH influence showed that MB dye on Cr/Fe<sub>3</sub>O<sub>4</sub>/CS

composite degraded fastest at pH=7. The color has been significantly reduced after the dye solution has been exposed to irradiation for a longer period of time, and the dye has been converted into organic material (COD test after 2h is low or under range). The kinetic research data support the first-order interpretation of MB dye degradation on Cr/Fe<sub>3</sub>O<sub>4</sub>/CS composite.

## Acknowledgements

Department of Chemistry, College of science, university of Baghdad and Prof. Dr. Khulood A. Saleh.

## Funding

This research did not receive any specific grant from funding agencies in the public, commercial, or not-for-profit sectors.

## Authors' contributions

All authors contributed to data analysis, drafting, and revising of the paper and agreed to be responsible for all the aspects of this work.

### Conflict of Interest

We have no conflicts of interest to disclose.

### ORCID:

Yaman Khalid Sadiq

<https://orcid.org/0000-0002-1651-786X>

### References

- [1]. Coleman, R.E., Boulton R.B., Stuchebrukhov A.A., Kinetics of autoxidation of tartaric acid in presence of iron, *The Journal of Chemical Physics*, 2020, **153**:064503 [[Crossref](#)], [[Google Scholar](#)], [[Publisher](#)]
- [2]. Kremer M.L., The Fenton reaction. Dependence of the rate on pH, *The Journal of Physical Chemistry A*, 2003, **107**:1734 [[Crossref](#)], [[Google Scholar](#)], [[Publisher](#)]
- [3]. Iurascu B., Siminiceanu I., Vione D., Vicente M.A., Gild A., Phenol degradation in water through a heterogeneous Photo-Fenton process catalyzed by Fe-treated laponite, *Water research*, 2009, **43**:1313 [[Crossref](#)], [[Google Scholar](#)], [[Publisher](#)]
- [4]. Ramirez J.H., Costa C.A., Madeira L.M., Mata G., Vicente M.A., Rojas-Cervantes M.L., LópezPeinado A.J., Martín-Aranda R.M., Fenton-like oxidation of Orange II solutions using heterogeneous catalysts based on saponite clay, *Applied Catalysis B: Environmental*, 2007, **71**:44 [[Crossref](#)], [[Google Scholar](#)], [[Publisher](#)]
- [5]. Coelho J.V., Guedes M.S., Prado R.G., Tronto J., Ardisson J.D., Pereira M.C., Oliveira L.C., Effect of iron precursor on the Fenton-like activity of Fe<sub>2</sub>O<sub>3</sub>/mesoporous silica catalysts prepared under mild conditions, *Applied Catalysis B: Environmental*, 2014, **144**:792 [[Crossref](#)], [[Google Scholar](#)], [[Publisher](#)]
- [6]. Sun L.J., Yao Y.Y., Wang L., Mao Y.J., Huang Z.F., Yao D.C., Lu W.Y., Chen W.X., Efficient removal of dyes using activated carbon fibers coupled with 8-hydroxyquinoline ferric as a reusable Fenton-like catalyst, *Chemical Engineering Journal*, 2014, **240**:413 [[Crossref](#)], [[Google Scholar](#)], [[Publisher](#)]
- [7]. Gao L., Zhuang J., Nie L., Zhang J., Zhang Y., Gu N., Wang T., Feng J., Yang D., Perrett S., Yan X., Intrinsic peroxidase-like activity of ferromagnetic nanoparticles, *Nature nanotechnology*, 2007, **2**:577 [[Crossref](#)], [[Google Scholar](#)], [[Publisher](#)]
- [8]. Xu L., Wang J., Fenton-like degradation of 2, 4-dichlorophenol using Fe<sub>3</sub>O<sub>4</sub> magnetic nanoparticles, *Applied Catalysis B: Environmental*, 2012, **123**:117 [[Crossref](#)], [[Google Scholar](#)], [[Publisher](#)]
- [9]. Guo L., Chen F., Fan X., Cai W., Zhang J., S-doped  $\alpha$ -Fe<sub>2</sub>O<sub>3</sub> as a highly active heterogeneous Fenton-like catalyst towards the degradation of acid orange 7 and phenol, *Applied Catalysis B: Environmental*, 2010, **96**:162 [[Crossref](#)], [[Google Scholar](#)], [[Publisher](#)]
- [10]. Su D., Yao M., Liu J., Zhong Y., Chen X., Shao Z., Enhancing mechanical properties of silk fibroin hydrogel through restricting the growth of  $\beta$ -sheet domains, *ACS applied materials & interfaces*, 2017, **9**:17489 [[Crossref](#)], [[Google Scholar](#)], [[Publisher](#)]
- [11]. Okumura Y., Ito K., The polyrotaxane gel: a topological gel by figure-of-eight cross-links, *Advanced materials*, 2001, **13**:485 [[Crossref](#)], [[Google Scholar](#)], [[Publisher](#)]
- [12]. Gong J.P., Why are double network hydrogels so tough?, *Soft Matter*, 2010, **6**:2583 [[Crossref](#)], [[Google Scholar](#)], [[Publisher](#)]
- [13]. Haraguchi K., Takehisa T., Nanocomposite hydrogels: a unique organic\_inorganic network structure with extraordinary mechanical, optical, and swelling/de-swelling properties, *Advanced materials*, 2002, **14**:1120 [[Crossref](#)], [[Google Scholar](#)], [[Publisher](#)]
- [14]. Hom W.L., Bhatia S.R., Significant enhancement of elasticity in alginate-clay nanocomposite hydrogels with PEO-PPO-PEO copolymers, *Polymer*, 2017, **109**:170 [[Crossref](#)], [[Google Scholar](#)], [[Publisher](#)]
- [15]. Al-Saade K.A.S., Al-Saidi S.F., Juad H.H., Degradation of Brilliant Green by Using a bentonite Clay-Based Fe Nanocomposite Film as a Heterogeneous Photo-Fenton Catalyst. *Baghdad Science Journal*, 2016, **13**:524 [[Crossref](#)], [[Google Scholar](#)], [[Publisher](#)]

- [16]. Shi X., Tian A., You J., Yang H., Wang Y., Xue X., Degradation of organic dyes by a new heterogeneous Fenton reagent-Fe<sub>2</sub>GeS<sub>4</sub> nanoparticle, *Journal of hazardous materials*, 2018, **353**:182 [[Crossref](#)], [[Google Scholar](#)], [[Publisher](#)]
- [17]. Kadhim H.H., Khulood A.S., Removing Cobalt ions from Industrial Wastewater Using Chitosan, *Iraqi Journal of Science*, 2022, 3251 [[Crossref](#)], [[Google Scholar](#)]
- [18]. Freire T.M., Dutra L.M., Queiroz D.C., Ricardo N.M.P.S., Barreto K., Denardin J.C., Wurm F.R., Sousa C.P., Correia A.N., Lima-Neto P., Fachine P.B.A., Fast ultrasound assisted synthesis of chitosan-based magnetite nanocomposites as a modified electrode sensor, *Carbohydrate polymers*, 2016, **151**:760 [[Crossref](#)], [[Google Scholar](#)], [[Publisher](#)]
- [19]. Muhi-Alden Y.Y., Saleh K.A., Removing of Methylene Blue Dye from its Aqueous Solutions Using Polyacrylonitrile/Iron Oxide/Graphene Oxide, *Iraqi Journal of Science*, 2022, **63**:2320 [[Crossref](#)], [[Google Scholar](#)], [[Publisher](#)]
- [20]. Foo K.Y., Hameed B.H., Insights into the modeling of adsorption isotherm systems, *Chemical engineering journal*, 2010, **156**:2 [[Crossref](#)], [[Google Scholar](#)], [[Publisher](#)]
- [21]. Yasser Yousef M.A.A., and Saleh K.A., Removing of Methylene Blue Dye from its Aqueous Solutions Using Polyacrylonitrile/Iron Oxide/Graphene Oxide, *Iraqi Journal of Science*, 2022, 2320 [[Crossref](#)], [[Google Scholar](#)]
- [22]. Vinu R., Madras G., Kinetics of sonophotocatalytic degradation of anionic dyes with nano-TiO<sub>2</sub>, *Environmental science & technology*, 2009, **43**:473 [[Crossref](#)], [[Google Scholar](#)], [[Publisher](#)]
- [23]. Arrhenius S., Über die Dissociationswärme und den Einfluss der Temperatur auf den Dissociationsgrad der Elektrolyte, *Zeitschrift für physikalische Chemie*, 1889, **4**:96 [[Crossref](#)], [[Google Scholar](#)], [[Publisher](#)]
- [24]. Freire T.M., Fachine L.M., Queiroz D.C., Freire R.M., Denardin J.C., Ricardo N.M., Rodrigues T.N.B., Gondim D.R., Junior I.J.S., Fachine P.B., Magnetic porous controlled Fe<sub>3</sub>O<sub>4</sub>-chitosan nanostructure: an ecofriendly adsorbent for efficient removal of azo dyes, *Nanomaterials*, 2020, **10**:1194 [[Crossref](#)], [[Google Scholar](#)], [[Publisher](#)]

#### HOW TO CITE THIS ARTICLE

Yaman Khalid Sadiq, Khulood A. Saleh. Synthesis and Characterization of Chrome (VI) ion/iron oxide/chitosan Composite for Oxidation of methylene blue by Photo-Fenton Reaction. *Chem. Methodol.*, 2023, 7(2) 112-122

<http://dx.doi.org/10.22034/CHEMM.2022.361921.1608>

URL: [http://www.chemmethod.com/article\\_159506.html](http://www.chemmethod.com/article_159506.html)